

REPRODUCING CRATER MORPHOLOGIES USING THE MELOSH MODEL OF ACOUSTIC FLUIDIZATION. A. Rajšić¹, B.C. Johnson^{1,2}, H.C.F.C. Hay³, G.S. Collins⁴. ¹Department of Earth, Atmospheric and Planetary Sciences, Purdue University, West Lafayette, Indiana, USA; ²Department of Physics and Astronomy, Purdue University, West Lafayette, Indiana, USA ³Department of Earth Sciences, Oxford University, UK; ⁴Department of Earth Science and Engineering, Imperial College London, London, SW7 2AZ, United Kingdom; (E-mail: arajsic@purdue.edu).

Crater collapse and acoustic fluidization: Impact craters on Earth larger than ~ 3 -6 km experience floor failure and wholesale gravitational collapse resulting in complex craters with flat floors, terraced rims, and central peaks [e.g., 1]. On the Moon, these craters occur at sizes larger than ~ 15 -20 km [2]. Theoretical studies showed that the strength of the rock needs to be 2-3 MPa, and with little or no friction, [e.g., 3, 4] to behave in the described way. This rheology departs significantly from measured rock strength, suggesting that some mechanism temporarily reduces strength during crater formation. Here, we use the Melosh model of acoustic fluidization [5] to explore target weakening during crater formation on Earth and the Moon.

The acoustic fluidization model was first proposed in 1979 by Melosh [5], and this description was successfully implemented into the iSALE-2D shock physics code by [6]. This model describes acoustic energy variation over time and space as a partial differential equation:

$$\frac{dE}{dt} = \frac{\xi}{4} \nabla^2 E - \frac{C_p}{\lambda Q} E + e \tau_{ij} \dot{\epsilon}_{ij} \quad (1)$$

where ξ is the scattering diffusivity, e is the regeneration parameter, Q is the dissipation quality factor, and λ is the wavelength of acoustic vibrations [7, 8]. This model accounts for the scattering/diffusion of the acoustic energy (the first term of the equation) and the conversion of acoustic energy into heat per unit of time (the second term). Finally, it includes the regeneration of acoustic energy via conversion of distortional energy per unit time ($\tau_{ij} \dot{\epsilon}_{ij}$).

An alternative version of the acoustic fluidization model, called the block model, is more often used in impact simulations owing to its slightly simpler implementation. The block model can successfully reproduce impact crater morphology on terrestrial [9] and icy bodies [10]. However, the block model does not account for the scattering and the regeneration of acoustic energy from equation 1 (i.e., $\xi=0, e=0$). Lack of acoustic energy regeneration might be why the block model fails to produce terraced rims [6, 11].

Here, we build on the efforts of [6] and conduct a detailed parameter investigation for the Melosh model of acoustic fluidization. We found a set of parameters (λ ,

Q , e) that successfully reproduce crater depth-to-diameter trends and crater morphology.

Numerical impact modelling: We simulate crater formation using iSALE-2D (<https://isale-code.github.io/>), a finite-difference shock physics code based on the SALE hydrocode [12]. Simulations are made assuming Earth's gravity field (9.81 m s^{-2}) and the Moon's gravity field (1.63 m s^{-2}). For impacts on Earth, impact velocity was 12 km s^{-1} , and impactor radii are varied between 0.036 km, and 7.2 km, to produce the full range of crater morphology (simple to peak ring craters). We use a strength model [13] and an ANEOS equation of state [14] for granite to represent the impactor and target material. On the Moon, we model target and impactor as in previous works [e.g., 15] using 15 km s^{-1} impactor speed and impactor radii between 0.25 km, and 25 km.

Previous work [1] showed that for the block model to produce the correct crater size, the dissipation quality factor needs to be between 10 and 100. Here, we vary Q between 10 and 400. The regeneration parameter (e) governs the conversion of shock energy to acoustic energy and energy regeneration. We test the regeneration factor between 0.025 and 0.1. In the block model [9], the block size is considered proportional to the impactor size. In the Melosh model, we adopt this assumption for acoustic vibration wavelength and vary λ between $0.01a$ to $0.5a$.

Results and Discussion: The Melosh model parameters (λ , Q , e) affect the duration and strength of the acoustic vibrations that control the reduction of target viscosity. We estimate the effective viscosity of fully fluidized material using the equation [7, 16]: $\eta = C_b h \rho$, where $C_b = 5500 \text{ m s}^{-1}$ (speed of sound in target); $\rho = 2630 \text{ kg m}^{-3}$ (density of the target), and $h = \lambda$ (block size in the block model, or wavelength of the vibrations in the Melosh model). We found that $\lambda = 0.2a$ gives the best agreement with the block model results.

We compare the effects of acoustic fluidization parameters on crater diameter (D) and depth-to-diameter ratios (d/D) (Fig. 1). Our smallest impactor produces a crater of $D \sim 2.4 \text{ km}$ and $d/D \sim 0.25$, and a simple, bowl-shaped morphology. Our mid-size impactor creates a central peak crater. This crater is $\sim 20 \text{ km}$ in diameter and has $d/D \sim 0.04$. The largest impactor makes a crater with an evident peak ring morphology with even lower d/D

($D \sim 140$ km, $d/D \sim 0.025$). For impact conditions shown in Fig. 1 the block model of acoustic fluidization produces $d/D \sim 0.24, 0.047, \text{ and } 0.029$, respectively (shown in blue). These predictions generally agree with our best-fit model (shown in red).

Crater morphology varies dramatically with the parameters used in the Melosh model. The product λQ controls the longevity of acoustic vibrations in the target. The degree of collapse is a trade-off between the longevity of acoustic vibrations and the effective viscosity of the acoustically fluidized rock. Fig. 1 shows the effect the dissipation factor (Q) has on the depth-to-diameter ratio for a fixed λ/a . All craters expressed complex crater morphology when $Q > 20$. However, reducing the regeneration parameter allows for a higher Q to be applied and achieve the desired depth-to-diameter ratio of terrestrial craters (red).

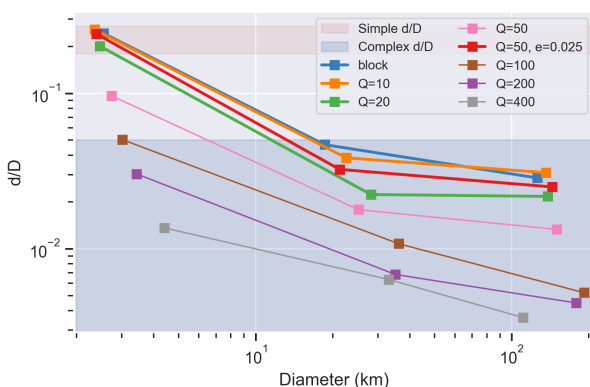


Figure 1: Depth-to-diameter ratio versus crater diameter measured in simulations with different quality factors. Simulations had constant $\lambda = 0.2a$ ($a = 0.072, 0.72, 7.2$ km). Our results indicate that above $Q = 20$, all craters express complex morphology (blue box).

Furthermore, we apply our best-fit Melosh model parameters (red, Fig 1) to various impact conditions on Earth and the Moon to observe the transition in crater morphology. Preliminary measurements (Fig. 2) of the final lunar crater depth and diameter (red squares) show agreement with the scaling trends [2] and measurements from previous works ([17] – red triangles). Final craters measured in simulations with Earth-like gravity (black squares) are in agreement with previous models [9] and show a transition from simple crater morphology at ~ 3.2 km.

Conclusion: For the right set of parameters, the Melosh model of acoustic fluidization reproduces similar d/D trends and crater morphologies as the block model on Earth and the Moon. The main parameters that control the longevity of acoustic vibrations and the viscosity

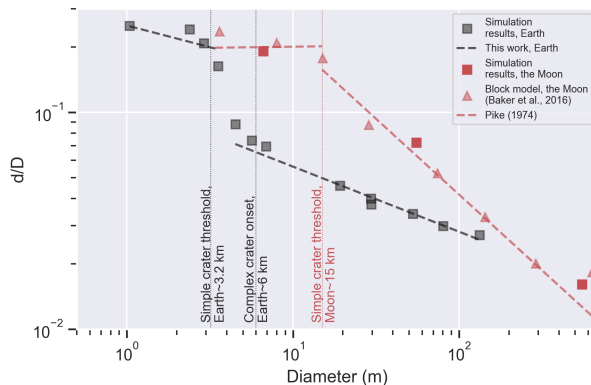


Figure 2: Preliminary measurements of the final crater depth and diameter on the Moon (red) and Earth (black). Our measurements show agreement with previous works.

of the target are the dissipation factor (Q) and the wavelength of the acoustic vibrations (λ). The target behaves too fluidly when the dissipation factor is $Q > 20$. However, lower values of the regeneration factor ($e = 0.025$) made it possible to increase the dissipation factor ($Q = 50$). For our best-fit Melosh model parameters, crater sizes in simulations made in Earth-like conditions show simple-to-complex transition at ~ 3.2 km. On the Moon, our initial results are comparable with previous works that used the block model.

Acknowledgements: We gratefully acknowledge the developers of iSALE (<https://isale-code.github.io/>). This work was partly supported by the NASA Lunar Data Analysis Program grant 80NSSC21K0048. GSC was supported by UK STFC grant ST/S000615/1.

References: [1] Melosh, H. & Ivanov, B. (1999) *Annual Rev. of Earth and Planet. Sci.* 385–415. [2] Pike, R. J. (1974) *Geophys. Res. Letters*, 1:291–294. [3] McKinnon, W. (1978) *LPSC* vol. 9. [4] McKinnon, W. & Melosh, H. (1978) *LPSC* vol. 9, 729–731. [5] Melosh, H. J. (1979) *J. Geophys. Res.* 84:7513–7520. [6] Hay, H. et al. (2014) *45th LPSC* 1777, 1938. [7] Collins, G. S. & Melosh, H. J. (2003) *J. Geophys. Res.* 108. [8] Melosh, H. (1996) *Nature*, 379:601–606. [9] Wünnemann, K & Ivanov, B. (2003) *Planetary Space Sci.* 51:831–845. [10] Bray, V. J. et al. (2014) *Icarus*, 231:394–406. [11] Kenkmann, T. et al. (2014) *J. Structural Geol.* 62:156–182. [12] Amsden, A. et al. (1980) tech. rep. Los Alamos Scientific Lab., NM (USA). [13] Collins, G. S. et al. (2004) *Meteoritics Planet. Sci.* 39:217–231. [14] Pierazzo, E et al. (1997) *Icarus*, 127:408–423. [15] Johnson, B. C. et al. (2016) *Science*, 354:441–444. [16] Ivanov, B. A. & Artemieva, N. A. (2002) *Spec. Paper of the Geol. Soc. of America*, 619–630. [17] Baker, D. M. et al. (2016) *Icarus*, 273:146–163.